Heliyon 9 (2023) e12888

Contents lists available at ScienceDirect

Heliyon

journal homepage: www.cell.com/heliyon

Research article

Prediction of methyl orange dye (MO) adsorption using activated carbon with an artificial neural network optimization modeling

Saja Mohsen Alardhi [a], Seef Saadi Fiyadh [b], Ali Dawood Salman [c,d,*], Mohammademad Adelikhah [e]

[a] Nanotechnology and Advanced Materials Research Center, University of Technology, Baghdad, Iraq
[b] Nanotechnology & Catalysis Research Centre (NANOCAT), IPS Building, University of Malaya, 50603 Kuala Lumpur, Malaysia
[c] Sustainability Solutions Research Lab, University of Pannonia, Egyetem str. 10, H-8200 Veszprem, Hungary
[d] Department of Chemical and Petroleum Refining Engineering, College of Oil and Gas Engineering Basra University, Iraq
[e] Institute of Radiochemistry and Radioecology, Research Centre for Biochemical, Environmental and Chemical Engineering, University of Pannonia, 8200 Veszprem, Hungary

ARTICLE INFO

Keywords:
Activated carbon
Adsorption capacity
Artificial neural network
Date stones
Methyl orange
Regression

ABSTRACT

In this study, methyl orange (MO) dye removal by adsorption utilizing activated carbon made from date seeds (DPAC) was modeled using an artificial neural network (ANN) technique. Instrumental investigations such as X-ray diffraction (XRD), scanning electron microscopy (SEM), and Brunauer-Emmett-Teller (BET) analysis were used to assess the physicochemical parameters of adsorbent. By changing operational parameters including adsorbent dosage (0.01–0.03 g), solution pH 3–8, initial dye concentration (5–20 mg/L), and contact time (2–60 min), the viability of date seeds for the adsorptive removal of methyl orange dye from aqueous solution was assessed in a batch procedure. The system followed the pseudo 2nd order kinetic model for DPAC adsorbent, according to the kinetic study (R2 = 0.9973). The mean square error (MSE), relative root mean square error (RRMSE), root mean square error (RMSE), mean absolute percentage error (MAPE), relative error (RE), and correlation coefficient (R^2) were used to measure the ANN model performance. The maximum RE was 8.24% for the ANN model. Two isotherm models, Langmuir and Freundlich, were studied to fit the equilibrium data. Compared with the Freundlich isotherm model (R^2 = 0.72), the Langmuir model functioned better as an adsorption isotherm with R^2 of 0.9902.

Thus, this study demonstrates that the dye removal process can be predicted using an ANN technique, and it also suggests that adsorption onto DPAC may be employed as a main treatment for dye removal from wastewater.

1. Introduction

One of the main dangers to our ecology, in one way or another, is aquatic pollution. Dye pollution poses the greatest damage to the environment among other pollutants including metal ions, dyes, insecticide sprays, etc. Because stable aromatic rings are present, dyes are toxic and non-biodegradable. Pollution can occur at very low concentrations, even ones of one ppm. Dye types include anionic, cationic, and non-ionic. They can induce allergic dermatitis, skin irritation, cancer, mutation, and other conditions in exposed

* Corresponding author. Sustainability Solutions Research Lab, University of Pannonia, Egyetem str. 10, H-8200 Veszprem, Hungary.
E-mail address: ali.dawood@mk.uni-pannon.hu (A.D. Salman).

https://doi.org/10.1016/j.heliyon.2023.e12888
Received 21 September 2022; Received in revised form 3 December 2022; Accepted 6 January 2023
Available online 10 January 2023

organisms, depending on their concentration and length of exposure. Researchers are experimenting with affordable and effective methods for their removal while taking the aforementioned factors into account [1].

The textile industry regularly uses the colorant methyl orange (MO). MO has been shown to be very hazardous, to damage the eyes, and could potentially result in long-term ocular harm [2]. Various techniques used for processes used in dye removal, These techniques include for example Ozonation [3], coagulation–flocculation [4], Photocatalytic oxidation [5] Algal treatment [6], Electrochemical oxidation [7], Membrane filtration [8], and adsorption [9–14]. Due to its adaptability, low cost, and simplicity of use, adsorption is regarded as the best wastewater treatment method. Both soluble and insoluble organic contaminants can be eliminated using adsorption. The elimination efficiency of this approach could reach 99.9%. These facts have led to the employment of adsorption in the removal of a range of organic contaminants from a number of contaminated water sources [15]. Adsorbents used in water remediation arise from either natural sources or are the product of industrialized manufacture and/or activation processes. Natural zeolites, clay minerals, biopolymers, or oxide are typical natural adsorbents [16]. Adsorbents have traditionally included activated carbon (AC), inorganic oxides, and natural materials such clays and clay minerals, chitin, cellulosic materials, and chitosan. Because of their extremely high surface areas, micro-pore volumes, significant adsorption capacities, quick adsorption kinetics, and generally simple regeneration processes, activated carbons (AC) are the most adaptable and widely utilized adsorbents [17]. The diverse waste products appear to be a desirable precursor for the manufacture of activated carbon. They are a readily available, affordable, environmentally friendly, and renewable source of raw materials and biomass [18]. The manufacturing of efficient activated carbons uses a wide range of waste products such as chickpea waste [19], sugar beet bagasse [20], tea waste [21], rice straw [22], coffee waste [23] and date seeds [24].

Modeling is a tried-and-true engineering technique that can aid in comprehension of the removal processes. However, because a wide range of trials are necessary, modeling removal processes by standard mathematical models (mechanistic models) is expensive and time-consuming. Additionally, wastewater treatment procedures are quite complicated and are influenced by a number of operating parameters and removal mechanisms. As a result, utilizing traditional mathematical models to model and improve the removal procedures is challenging. Recent trends advocate the use of empirical models, such as artificial neural networks, to model wastewater treatment processes [25].

Artificial neural network is frequently utilized as alternative mathematical methods to tackle many issues with modest changes. Researchers are encouraged to use nonlinear models like artificial neural networks for the prediction of the adsorption profile since the adsorption process is complex and nonlinear [26].

The aim of this work is to create date seed-based activated carbon as an adsorbent for the removal of MO dye from aqueous solution. In this investigation ANNs were utilized to forecast the MO dye adsorption on date-seed-derived activated carbon. Four parameters, including pH, adsorbent dosage, adsorption time, and initial dye solution concentration, were examined for their effects on the of MO dye adsorption. The results were then modeled using ANN. Additionally, the adsorption of the MO dye on activated carbon was examined using isotherm and kinetics models.

To our knowledge, the removal of methyl orange dye by activated carbon made from date seeds (DPAC) using an artificial neural network (ANN) technique has never been investigated.

2. Materials and methods

2.1. Materials

Analytical-grade chemical reagents were purchased from Sigma-Aldrich for laboratory studies. Methyl Orange dye (MO) was used as model dye (molecular weight: 327.34 g mol^{-1} with molecular formula of $C_{14}H_{14}N_3NaO_3S$). Fig. 1 presented chemical structure of methyl orange. Phosphoric acid (H_3PO_4) was used for adsorbent impregnation. Hydrochloric acid (37%) (HCl), Sodium Hydroxide (NaOH) were used for the pH adjustment. All reagents were used without further purification.

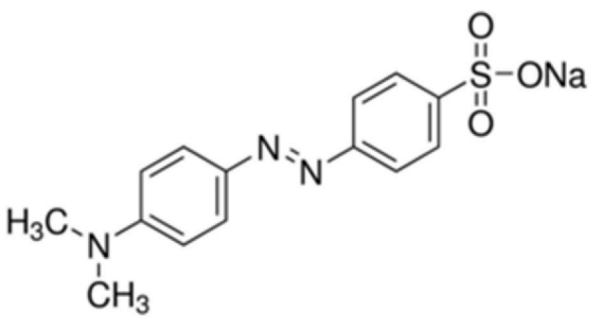

Fig. 1. Chemical structure of methyl orange.

2.2. Synthesis of activated carbon adsorbent

As an adsorbent, activated carbon was prepared in accordance with (Essa, 2008) [27] as shown in Fig. 2. Date seeds were gathered, cleaned, and dried for 48 h at 120 °C in an air furnace before being crushed and sieved. Utilizing phosphoric acid, the resultant sieve is utilized to prepare activated carbon through chemical activation. The reaction took place for 2 h at 100 °C, and the final sample was dried in an oven. The impregnated material was pyrolyzed in a cylindrical stainless steel reactor. Pyrolysis time was maintained for 4 h at a temperature of 500 °C. The produced activated carbon was repeatedly rinsed with hot distilled water until neutral pH was reached, then allowed to cool to room temperature. The prepared DPAC were cooled for room temperature, dried and finally kept for subsequent uses. Table 1 shows the properties of the DPAC used as an adsorbent in this study.

2.3. Characterization

X-ray diffraction (XRD) (XRD-6000, Shimadzu, Japan); the X-ray source releases radiation at a wavelength of 0.15405 nm; was used to describe the structure of the DPAC made from date seeds. The system runs at 60 kV with an emission current of 80 mA. Scanning electron microscopy (SEM) was used to analyze the morphology of the adsorbent (Tescan VEGA 3 SB, SEM). The specific surface area of AC was measured using nitrogen adsorption isotherm data at 77 K utilizing the Brunauer, Emmett, and Teller (BET).

2.4. Methyl orange dye adsorption runs

In 1L of distilled water, 1 g of MO was added to create the stock solution (1000 mg/L), to obtain the appropriate concentration. A variety of concentrations will be examined in the experiment and ranging from (5, 10, 20, 30 ppm) for preparation of the calibration curve. At a wavelength of 450 nm, the absorbance of each concentration was measured. The residual concentration after treatment was then determined by plotting each concentration against the absorbance and using the resulting equation. The effectiveness of MO dye adsorption on the DPAC adsorbent was investigated using a variety of parameters, including pH, adsorbent dosage, initial dye solution concentration, and adsorption time. The pH, adsorbent dosage, initial solution concentration, and adsorption duration ranges that were examined were 3–8, 0.01–0.03 g, 5–20 mg/L, and 2–60 min, respectively. The dye concentration was determined using visible light spectroscopy with a maximum wavelength of 450 nm. Each experiment involved stirring 50 mL of MO dye solution with a specific initial concentration, pH, and amount of adsorbent. After filtering the resultant solution, visible light spectroscopy was used to determine the final concentration. The following equation was used to get the dye adsorption efficiency:

$$\%Removal = \frac{C_i - C_e}{C_i} \times 100 \tag{1}$$

Where C_i and C_e (mg/L) represent the initial and equilibrium adsorbate concentrations, respectively.

Equation (2):

$$q_e = \frac{(C_i - C_f)\, V}{M} \tag{2}$$

where q_e (mg. g^{-1}) is the capacity of adsorption at the adsorbent equilibrium, C_f (mg. L^{-1}): initial final concentration of MO dye, correspondingly, M (g) is the used adsorbents quantity and V (L) is the volume of solution.

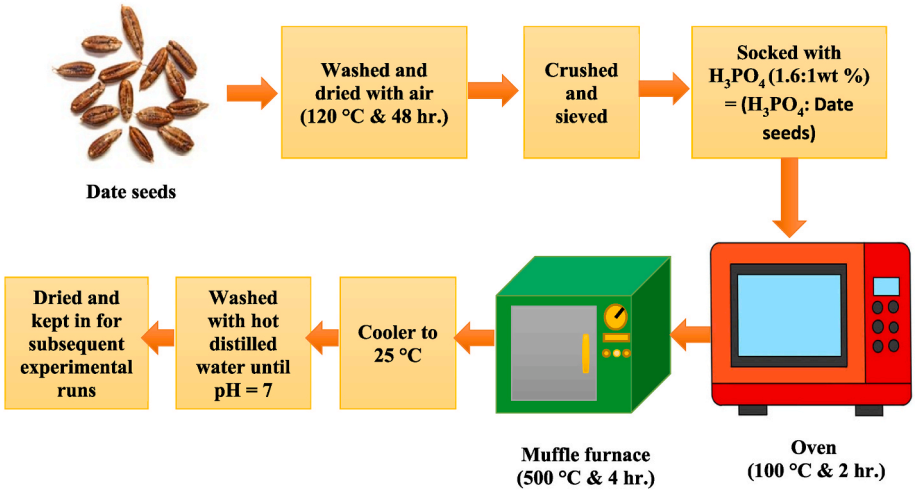

Fig. 2. Process flow diagram for prepared DPAC from date seeds.

Table 1
Physical properties of DPAC from date seeds.

Property	Value
Specific Surface area	520 m^2/g
Pore volume	0.36 cm^3/g
Real density	2.8 g/cm^3
Color	black

2.5. Isotherm and kinetics studies

The adsorption isotherms' goal is to connect the concentration of equilibrium dye molecules at the solid surface to that in the bulk solution [28]. The isotherm data must be proportioned correctly to the several isotherm models in order to generate the fit model used in the design phase [29].

Two isotherm models used in this study: Langmuir and Freundlich adsorption models linear form are given in Table 2; Kinetic and equilibrium behavior are the characteristics that define adsorption processes. Adsorption kinetics was examined in order to better understand the dynamics of MO dye adsorption onto DPAC. To examine the process' adsorptive behavior, adsorption kinetic models were used [30]. Numerous liquid phase kinetic models have been employed to explain experimental data. Pseudo-first-order, pseudo-second-order, and other models are among them. For more details, see Table 2 for an investigation using equations into the kinetics and diffusion of the MO adsorption onto the DPAC adsorbent. The experimental steps of the isotherm and kinetics models are present in Fig. 3.

2.6. Artificial neural networks

Relationships in challenging nonlinear data sets have been widely achieved using artificial neural network models. ANN models have been adopted successfully in a variety of environmental engineering issues [33]. Input layer, hidden layer, and output layer are the three layers that make up most ANN models (Fig. 4). Neurons, which are basic processing units, make up each layer. Neurons transmit information between layers via weighted signals. Outside sources send signals to the input layer. This layer applies weighting to each input separately before sending the data to the hidden layer for processing [34]. Preprocessing was carried out using hidden layers, and the outcomes were then moved via transfer functions into additional hidden layers and output layers [32]. The feed forward neural network can only move data forward in one direction [34]. In this work, an ANN was created using four parameters to determine the removal effectiveness of the MO dye using DPAC. To have effective ANN training, it is essential to make sure that the data set appropriately covers the variables. If not, the model can fail the generalization test and be only useful for the specific set of parameters that the experimental data illustrate. The input and output parameter ranges given to a network are shown in Table 3. The results were compared to experimental ones. The trained ANN was always used to estimate the removal efficacy of MO dye in varied situations that were not used for training (testing data). The input nodes of the ANN model include pH, adsorbent dose, initial concentration, and contact time, while the output node is removal efficiency of MO dye. To train the ANN model, 100 test runs were carried out [2]. Table 4 summarizes and presents the ANN model's applications for estimating dye adsorption.

Several indices, as well as the anticipated and actual outcomes, were used in this study to test the reliability of the ANN models. RRMSE, MAPE, MSE, RMSE, and RE are these markers.

$$RRMSE = \left[\frac{1}{n}\sum_{t=1}^{n}\left(\frac{D_a(t) - D_f(t)}{D_a(t)}\right)^2\right]^{\frac{1}{2}} \tag{3}$$

$$MSE = \frac{1}{n}\sum_{i=1}^{n}\left(D_a(t) - D_f(t)\right)^2 \tag{4}$$

Table 2
Isotherm and Kinetic models used to fit the adsorption of methyl orange (MO) on DPAC.

Type of Models		Equations	Parameters	Refs.
Adsorption Isotherm Models	Langmuir	$\frac{C_e}{q_e} = \frac{1}{q_{max}}C_e + \frac{1}{q_{max}\ b}$	C_e (mg·L $^{-1}$): equilibrium concentration of the MO in the solution q_e (mg·g $^{-1}$): removed amount of MO at equilibrium. q_{max} (mg·g $^{-1}$): maximum adsorption capacity, b (L·mg^{-1}): Langmuir constant	
	Freundlich	$ln\ q_e = ln\ K_f + \frac{1}{n} ln\ Ce$	K_F (mg/g)/(mg/L)$^{1/n}$: MO adsorption capacity. n: heterogeneity factor.	
Adsorption Kinetics Models	Pseudo-first-order	$\log(q_e - q_t) = \log q_e - \frac{K_1}{2.303}\ t$	q_t (mg·g $^{-1}$): removed amount of MO at time t. qe (mg·g $^{-1}$): equilibrium adsorption uptake K_1 (min−1): rate constant of the first-order adsorption.	[31]
	Pseudo-second-order	$\frac{t}{q_t} = \frac{1}{K_2\ {q_e}^2} + \frac{1}{q_e}\ t$	K_2 (g mg^{-1} min^{-1}): rate constant of the second-order adsorption	[32]

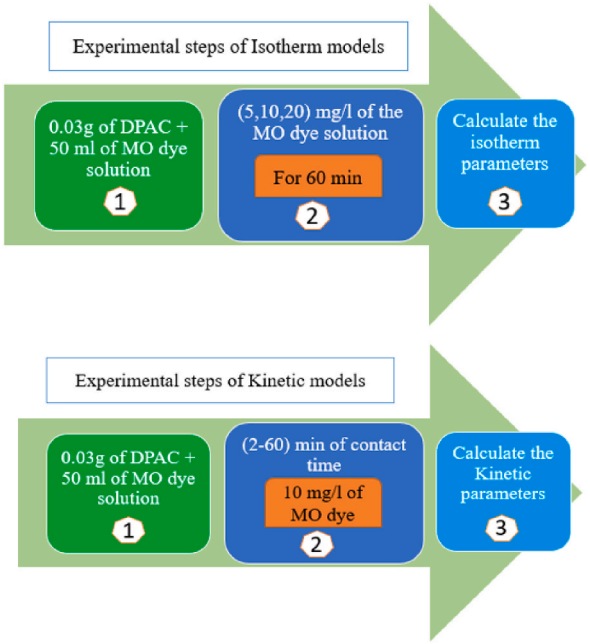

Fig. 3. The experimental steps of the isotherm and kinetics models.

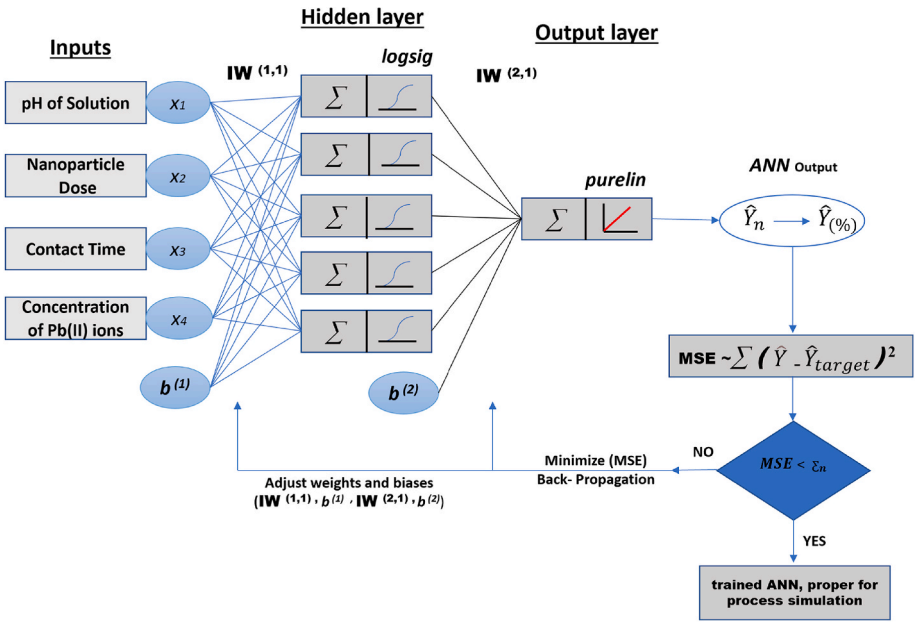

Fig. 4. Artificial neural network structure.

Table 3
Variables used in the ANN model's experimental range and levels.

Type	Variables	Range
Inputs	pH	3–8
	Time (min)	2–60
	DPAC dose (g)	0.01–0.03
	MO Concentration (mg/L)	5–20
Outputs	Removal efficiency (%)	15.3–99.82

Table 4
An overview of studies on dye adsorption modeling.

Type of Dye	Type of Adsorbent	Optimal number of neurons	References
Methyl orange	Chitosan/Al_2O_3/Fe_3O_4 core-shell composite microsphere	2-8-1	[35]
Crystal violet	Magnetic activated carbon	5-8-1	[36]
Basic Red 18	CuO–NiO nanocomposite	3-11-1	[37]
Basic Blue 41		3-10-1	
Ethidium bromide	Natural pumice and iron-coated pumice	4-2-2-1	[38]
		4-1-2-1	
Methyl orange	Gold nanoparticles-activated carbon Tamarisk	3-11-1	[39]
		3-20-1	
Methylene blue	Activated spent tea (AST)	5-10-1	[40]

$$RMSE = \left[\frac{1}{n}\sum_{t=1}^{n}\left(D_a(t) - D_f(t)\right)^2\right]^{\frac{1}{2}} \tag{5}$$

$$MAPE = \frac{1}{n}\sum_{t=1}^{n}\left|\frac{\left(D_a(t) - D_f(t)\right)}{D_a(t)}\right| \times 100 \tag{6}$$

$$RE = \frac{D_a(t) - D_f(t)}{D_a(t)} \times 100 \tag{7}$$

Where: $D_a(t)$ and $D_f(t)$ are the actual and predicted values at time t.

The indices utilized to assess model performance were RRMSE, MSE, RMSE, MAPE, and RE. Utilizing several indicators served to verify the model's accuracy. By examining the discrepancy between the actual and predicted outcomes, all indicators were based on the results that were attained.

3. Results and discussion

3.1. X-ray diffraction (XRD), SEM and FTIR

Phase purity was investigated by XRD technique. As described in section 2.2, XRD patterns of date seed particles activated with phosphoric acid are shown in Fig. 5. The broad diffraction peak seen at $2\theta = 22^{\circ}$ represents the graphite crystallinity in sample. The fact that there was no characteristic peak in the DPAC made the adsorbent's amorphous nature very obvious. The amorphous nature of the adsorbent makes it easier for pollutants to diffuse to its surface, which would result in an efficient removal of pollutants [41]. The broad peaks for DPAC may be seen between angles (2Θ) of 20^{o} and 27^{o} on the XRD graph. Broad peaks in the XRD pattern reflect the

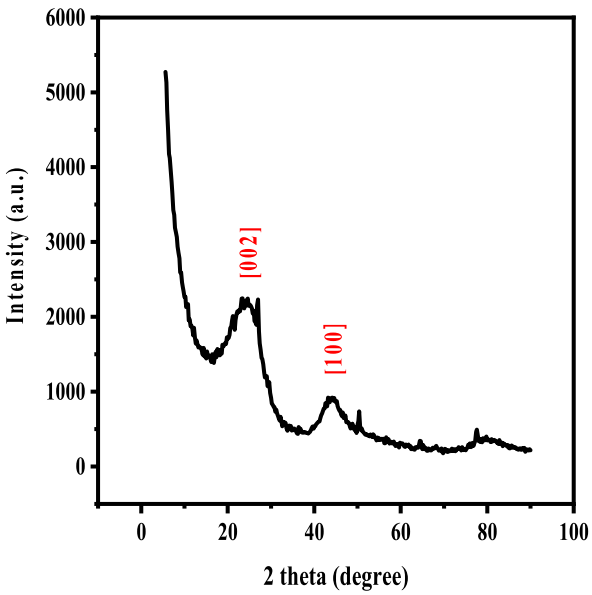

Fig. 5. XRD patterns of DPAC adsorbent.

activated carbon's amophous nature, whereas pointed peaks denote the crystalline nature [42]. This shows that DPACs exclusively include carbon materials with certain oxygenated functional groups, which is a useful feature of activated carbon for adsorption.

Scanning electronic microscopy was used to examine the surface morphology of DPAC, as present in Fig. 6). DPAC's surface had a crooked appearance before adsorption, with holes and voids visible. Fig. 7 shows the FTIR spectra of DPAC adsorbents before and after adsorption process.

3.2. The effect of solution pH

The pH has an effect on the surface charge of the adsorbent, the activity of functional groups, the competition with other ions in the solution, and the chemistry of the contaminated solution. The aqueous medium's pH can have an impact on the adsorbent's properties, the adsorption process, and the dissociation of dye molecules. The pH of the solution can change not just the adsorbent but also the chemical structure of the dye. The pH alters degree of ionization and the adsorbed ion's surface charge as shown in Fig. 8 [43,44].

Fig. 9 showed that the percentage of adsorption declined as pH increased, starting at pH equal to 3, which is the maximum value, and reaching its minimum value at pH equal to 5. And after that, as the pH rises, the proportion of adsorption also rises until it reaches pH 8 or above. The reason behind that could be due to the precipitation of the sodium salt of methyl orange. The high pH solution also eliminates the possible phenol formed by conversion in the water soluble phenoxide anion.

Because of its impact on the surface properties of the adsorbent and the dissociation/ionization of the adsorbate molecule, the adsorptive adsorption of adsorbate molecules is significantly influenced by the pH of the solution. Due to the interaction between the dye and the extra H^+ ions in the dye solution, the amount of dye that is adsorbed increases as pH values decrease [45,46].

3.3. Effect of adsorbent dosage

Adsorbent dosage is a key factor in adsorption that affects both the economics of the operation and the amount of removal. Initial MO concentration of 10 mg/L with a pH adjustment of 8, different amounts of DPAC from 0.01 to 0.03 g were employed at room temperature and 10 min contact time to examine the effect of adsorbent dosage of DPAC adsorption. More adsorption sites are available for MO dye molecules with increasing adsorbent dosages. As seen in Fig. 10, as the adsorbent dosage increased from 0.01 to 0.03 g, the adsorption capacity decreased from 6.6 to 1.8 mg/g. Due to more active sites of the adsorbent remaining unsaturated during the MO dye adsorption process, the adsorption capacity decreased with an increase in the adsorbent dosage of DPAC [1,47,48].

3.4. Effect of initial dye concentration

The effect of the MO dye initial concentration on the adsorption capacity was investigated by fixing a contact time of 10 min, adsorbent dosage of 0.03 g and pH of 8. The adsorption capacity increased along with the dye concentration in the water solution. The adsorption capacity was 0.63 mg/g at a 5 mg/L ion concentration; however, when the ion concentration was increased to 10 and 20 mg/L, the adsorption capacity increased to 2.06 mg/g and 6.17 mg/g, respectively. The improvement in adsorption capacity with

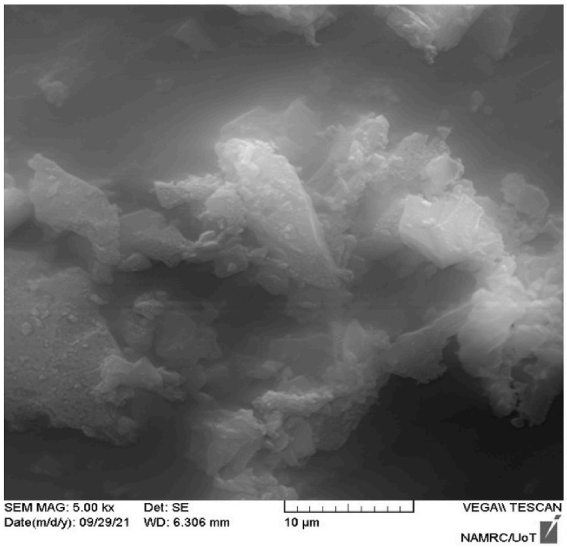

Fig. 6. SEM image of DPAC sample.

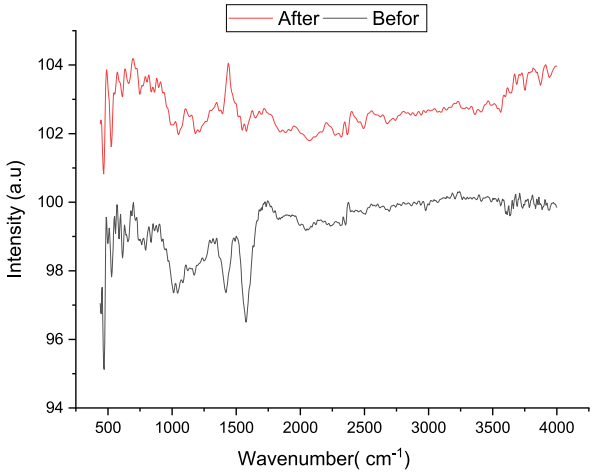

Fig. 7. FTIR spectra of DPAC adsorbents before and after adsorption.

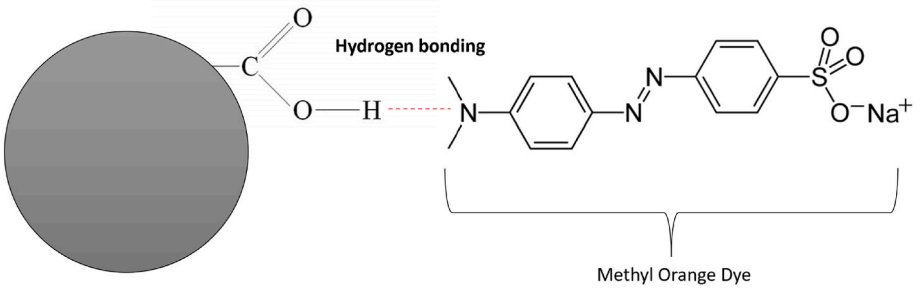

Fig. 8. Interaction mechanism between MO dye and DPAC.

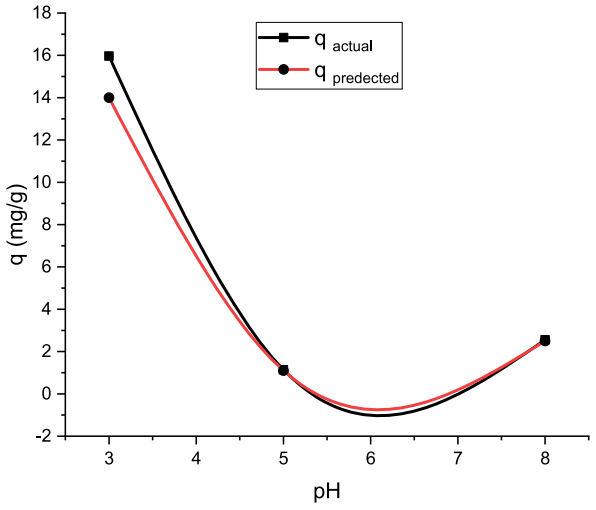

Fig. 9. Effect of pH on the removal of MO by DPAC at 25 °C (0.03 g, 10 mg/L dye solution).

increasing ion concentration can result in a greater active site occupancy and adsorption capacity because of the higher collision probability between the adsorbent active sites and the adsorbent molecules. The obtained experimental data were used to train the ANN model. The predictions made by the ANN model and the experimental data agreed well. Fig. 11 displays the experimental and ANN outcomes.

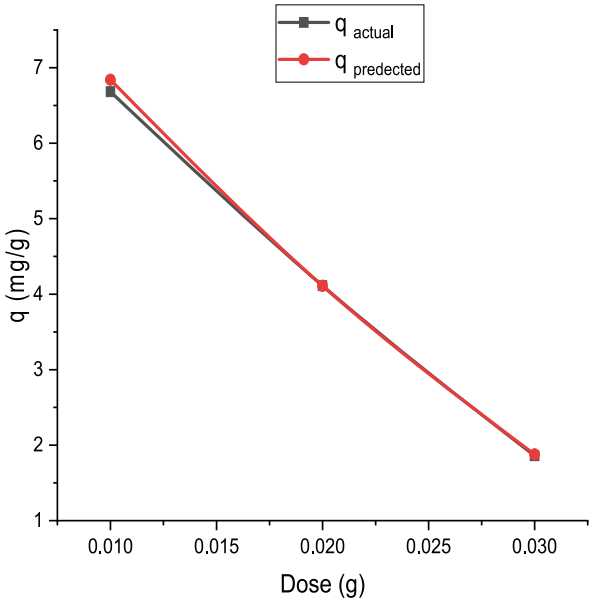

Fig. 10. Effect of adsorbent dosage and MO dye removal using AC (pH = 8, 25 °C temperature, 10 min and 10 mg/L initial concentration of the dye).

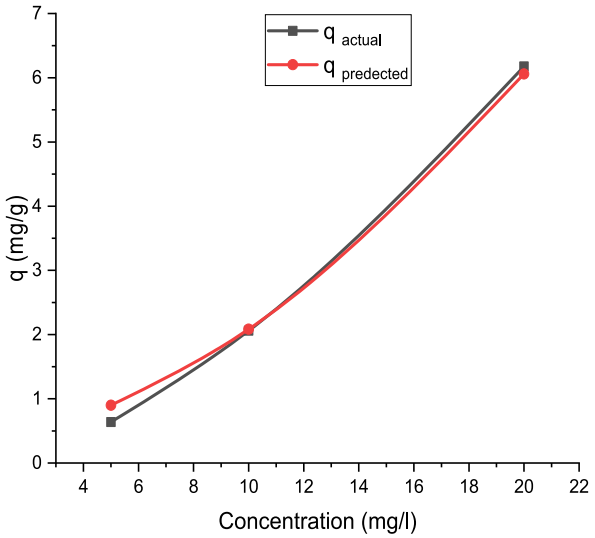

Fig. 11. Effect of initial dye concentration on DPAC performance separation (pH = 8 and 25 °C temperature).

3.5. Effect of contact time

Adsorbate molecules can diffuse and adhere during the contact time, which is a critical component of the adsorption process. This experiments, which was conducted at 2–60 min with pH 8, concentration of 10 mg/L, and amount of adsorbent 0.03 g, aimed to determine the optimum contact time. According to Fig. 12, the optimum contact time is 60 min, with an uptake capability of 2.7 mg/g. Due to the equilibrium condition occurring at 60 min till the completion of the experiment, the adsorption rate slows down over time.

3.6. Isotherm study

The adsorption isotherms' goal is to connect the concentration of equilibrium dye molecules at the solid surface to that in the bulk solution. All parameters were established and reported in Table 5 to explain the interaction of MO dye with DPAC using the Langmuir and Freundlich adsorption models. The correlation coefficient R^2 was used to assess the isotherm's suitability to explain the adsorption process. In this study Langmuir isotherm model was best fitted for DPAC (Fig. 13). The Langmuir isotherm makes the assumption that

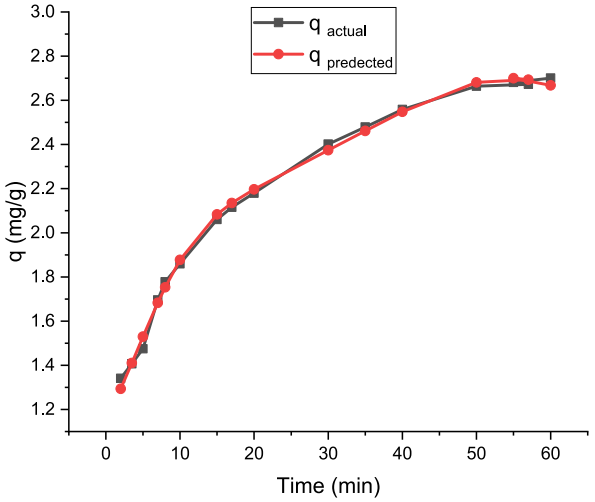

Fig. 12. Effect of contact time on DPAC performance separation (pH = 8 and 25 °C temperature).

Table 5
Isotherm model for adsorption of MO dye.

Adsorbent	Langmuir Isotherm			Freundlich Isotherm	
	q_m (mg/g)	KL (L/mg)	R^2	K_F (L/mg)	R^2
ACDP	7.57	0.930	0.9902	5.44	0.72

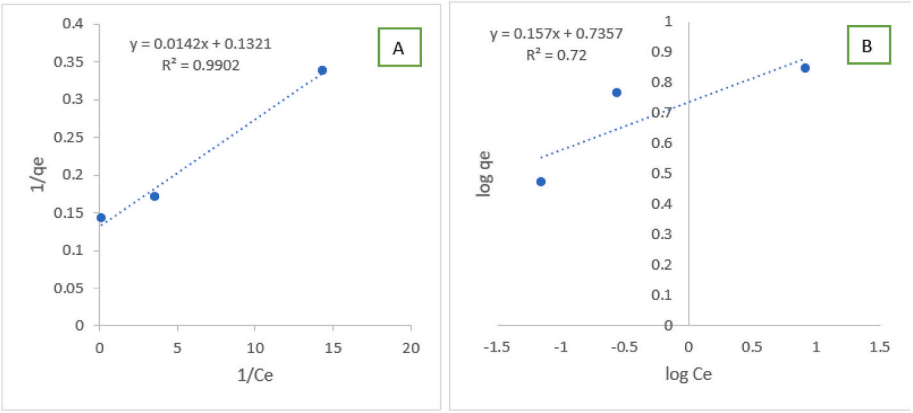

Fig. 13. (A) Langmuir model and (B) Freundlich model for MO adsorption.

the adsorbate is covered in a monolayer on the homogenous adsorbent surface, and that each molecule on the surface has an equal amount of adsorption activation energy.

3.7. Adsorption kinetics

The DPAC adsorbent was used in the kinetic investigation to track the behavior of the reaction. Three well-known kinetic models—pseudo-first-order, pseudo-second-order, and intraparticle diffusion models—were used. Fig. 14 shows the results of a pseudo 2nd order kinetic investigation with an initial MO dye concentration of 10 mg/L, a pH of 8, and various time intervals until equilibrium. Results of a pseudo 2nd order kinetic investigation utilizing an adsorbent dosage of 0.03 mg, an initial concentration of 20 mg/L, a pH of 8, and a contact period (time to equilibrium) of 60 min are shown in Fig. 15. Based on the results presented in Figs. 14 and 15, the DPAC adsorption kinetics fit the pseudo-second order model with a higher correlation coefficient R^2 value than that obtained for the intraparticle diffusion and pseudo first-order models. Table 5 displays the outcomes of pseudo first-order and the intraparticle diffusion models. The experimental results were predicted and modeled using the ANN approach. The ANN outputs were also subjected to the

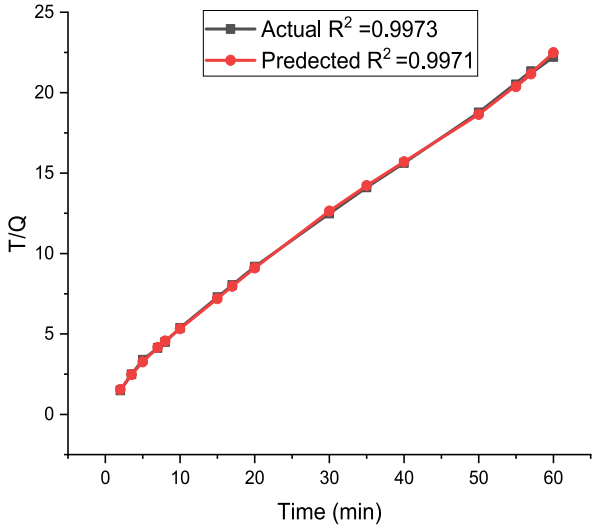

Fig. 14. Pseudo 2nd order Kinetic study at (adsorbent dosage of 0.03 g, MO dye initial concentration of 10 mg/L, pH of 8).

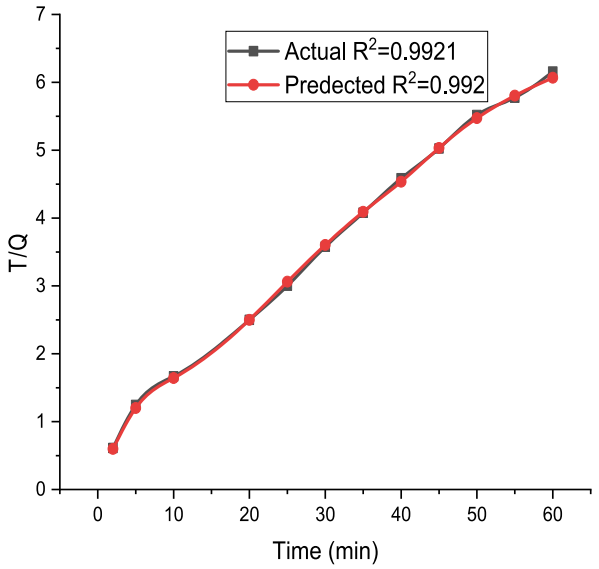

Fig. 15. Pseudo 2nd order Kinetic study at (adsorbent dosage of 0.03 g, MO dye initial concentration of 20 mg/L, pH of 8).

three kinetic models used to simulate the experimental data. Compared to the intraparticle diffusion and pseudo first-order models, the pseudo second-order model provided a superior description of the adsorption kinetics in this investigation. With R^2 values more than 0.99 at various initial concentrations, the kinetics study's findings matched the pseudo-second-order model. With an R^2 value more than 0.99 under the identical conditions, the ANN output result was likewise fitted to the pseudo-second-order model, demonstrating that the ANN model is in good agreement with the experimental findings. This agreement attests to the ANN model's high degree of accuracy. The kinetic results are presented in Table 6. Table 7 shows the ANN architecture optimization.

Table 6
Adsorption kinetics and correlation coefficients.

Experimental conditions			Pseudo first-order $\ln(q_e-q_t)$ *vs time (t)*		Pseudo second-order $(t/q_t$ *vs t)*		Intraparticle $(q_t$ *vs* $t^{0.5})$	
Dose mg	pH	C_0 mg/L	Experimental R^2	ANN output R^2	Experimental R^2	ANN output R^2	Experimental R^2	ANN output R^2
0.03	8	10	0.9733	0.9085	0.9973	0.9971	0.9694	0.9674
0.03	8	20	0.9308	0.9657	0.9921	0.992	0.9371	0.9253

Table 7
ANN architecture optimization.

Try	Number of neurons	Number of hidden layer	MSE	R^2
1	8	3	0.0038546	0.9815
2	10	3	0.005457	0.9763
3	12	3	0.005621	0.792
4	14	3	0.00596	0.961
5	8	2	0.000421	0.985
6	**10**	**2**	**0.000296324**	**0.9971**
7	12	2	0.000549	0.983
8	14	2	0.009521	0.9895

3.8. Neural network performance

By using MATLAB R2021a software, ANNs were used to model the removal of MO dye from simulated waste water using the DPAC adsorbent. In order to estimate the adsorption capacity of the DPAC adsorbent, the neural network was given the experimental data set obtained at the lab scale with a total of 100 data points. A number of variables, including adsorbent dosage (0.01, 0.02, and 0.03 g), pH (3, 5, and 8), MO dye concentration (5, 10 and 20 mg/L), and contact period (2–60 min), were first included in the experimental study and then later incorporated in the modelling. At the lab scale, one hundred (100) datasets were created. Twenty-five (25) records were used for testing, and 75 records were used for training and validating the network.

In this study, FFNN were utilized for kinetic investigations as well as to examine the effects of variables including pH, adsorbent dose, and initial concentration. The optimum structure was selected in this study is based on try and error method. The optimum structure is by using 2 hidden layers with 10 neurons in each hidden layer whereby, the first layer (inputs layer) 4 neurons are used which is based on the 4 parameters that used in this study (contact time, adsorbent dosage, pH, and initial concentration), one neuron is used for the output layer (adsorption capacity). Maximum RE for the FFNN model is 8.240% (Fig. 16), and R^2 is 0.9971 (Fig. 17).

It is difficult to choose a model structure with high accuracy and predictability since so many variables must be taken into account, including the number of hidden layers, the neurons in each layer, and the type of transfer function. In this work, the optimal network topology was chosen based on network productivity and performance, and different numbers of nodes, hidden layers, and transfer function types were used. The performance of the developed neural network model was evaluated based on the testing set using various indicators, using the starting MSE value from the training step; the results are shown in Table 8.

3.9. Comparative study

Food waste items among the biosorbents seemed to remove contaminants from wastewater effectively. Numerous advantages of biosorption from food waste include free availability, low production costs, and the potential for biosorbents to be recycled. Additionally, it is crucial to utilise waste as a sustainable supply of biomass for new goods and applications. With accompanying environmental and financial benefits, using such residual materials for wastewater treatment may become an effective option. Table 9 shows that when compared to similar type of materials, the MO dye was removed with the highest percentage.

4. Conclusion

With the use of ANN modelling, the DPAC was able to successfully absorb dye molecules from aqueous solution. It was investigated several parameters, such as the concentration of MO dye, pH, adsorbent dose, and contact time, affected each other. At pH 8, dosage 0.03 g, and dye concentration 10 mg/L, the best elimination was achieved. Lab tests revealed an optimal adsorption capacity of 2.6 1.0%, which was similar to the value anticipated by the ANN model. Three kinetics models were applied to the actual and predicted data: pseudo first-order, pseudo second-order, and intraparticle diffusion models. The second-order model developed using ANN

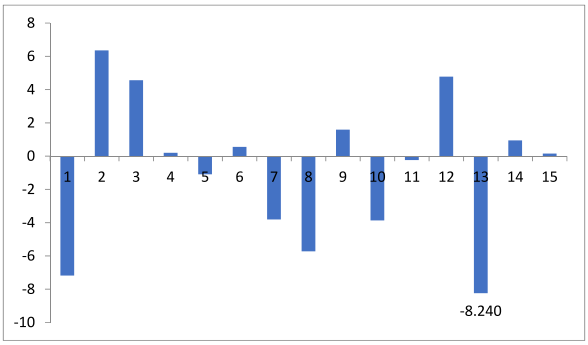

Fig. 16. Relative error (RE) of the FFNN model.

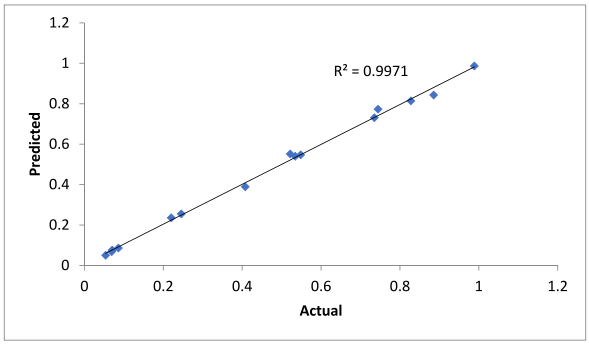

Fig. 17. Coefficient of correlation (R^2) of the neural network model.

Table 8
Performance indicators.

Indicator	FFNN
MSE	0.000296324
RMSE	0.017214061
RRMSE	0.04249035
MAPE	3.28%

Table 9
Comparative Analysis of prepared Activated Carbon from different west sources for MO dye removal.

Source of AC	Kinetic Study	Isotherm Study	Efficiency (%)	Reference
AC from Date Stones	Pseudo-second-order	Freundlich Isotherm	76.6	[2]
AC from Prickly Pear Seed Cake	Pseudo-second-order	Freundlich Isotherm	–	[49]
AC from coffee grounds	–	Freundlich Isotherm	60–65	[50]
AC from popcorn	Pseudo-second-order	–	48.5	[51]
AC from waste tire rubber	Pseudo-second-order	Langmuir Isotherm	80	[52]
AC made from date seeds	Pseudo-second-order	Langmuir Isotherm	99.82	This study

Bold values signifies the best results.

effectively modeled the impacts of the chosen variables in the dye removal process. The maximum RE, R^2, and MSE for the FFNN model were 8.24%, 0.9971, and 3.5995 10^{-5}, respectively. According to the study's findings, color removal from wastewater used in the textile sector might be accomplished through adsorption on DPAC, which would lower the cost of additional treatment.

Author contribution statement

Saja Mohsen Alardhi: Conceived and designed the experiments; Wrote the paper.
Seef Saadi Fiyadh: Performed the experiments; Wrote the paper.
Ali Dawood, Ph.D.: Analyzed and interpreted the data; Wrote the paper.
Mohammademad Adelikhah: Contributed reagents, materials, analysis tools or data.

Funding statement

This research did not receive any specific grant from funding agencies in the public, commercial, or not-for-profit sectors.

Data availability statement

Data will be made available on request.

References

[1] H. Radnia, A.A. Ghoreyshi, H. Younesi, G.D. Najafpour, Adsorption of Fe(II) ions from aqueous phase by chitosan adsorbent: equilibrium, kinetic, and thermodynamic studies, Desalination Water Treat. 50 (1–3) (2012) 348–359, https://doi.org/10.1080/19443994.2012.720112.
[2] S. Mitra, T. Mukherjee, P. Kaparaju, Prediction of methyl orange removal by iron decorated activated carbon using an artificial neural network, Environ. Technol. 42 (21) (2021) 3288–3303, https://doi.org/10.1080/09593330.2020.1725648.

[3] N.A. Razali, C.Z. Azner Abidin, O. Soon An, F. Muhammad Ridwan, A. Haqi Ibrahim, S.N. Sabri, S.H. Kow, Preliminary screening oxidative degradation methyl orange using ozone/persulfate, in: E3S Web Conf., vol. 34, 2018, 02038.

[4] Y.-Y. Lau, Y.-S. Wong, T.-T. Teng, N. Morad, M. Rafatullah, S.-A. Ong, Degradation of cationic and anionic dyes in coagulation–flocculation process using bi-functionalized silica hybrid with aluminum-ferric as auxiliary agent, RSC Adv. 5 (43) (2015) 34206–34215, https://doi.org/10.1039/C5RA01346A.

[5] V. Vaiano, G. Iervolino, Photocatalytic removal of methyl orange azo dye with simultaneous hydrogen production using Ru-modified ZnO photocatalyst, Catalysts 9 (11) (2019) 964.

[6] S.J. Anwar, I.U.H. Bhat, H.M. Yusoff, M.H. Razali, M.A. Kadir, L.K. Ern, Brown algae-based preparation, characterization and application of Pd nanocatalyst for enhanced reductive azo dye degradation, Clean. Engin. Techn. 4 (2021), 100172, https://doi.org/10.1016/j.clet.2021.100172.

[7] H. Yang, J. Liang, L. Zhang, Z. Liang, Electrochemical Oxidation Degradation of Methyl Orange Wastewater by Nb/PbO2 Electrode, 2015.

[8] A.M. Hidalgo, G. León, M. Gómez, M.D. Murcia, E. Gómez, J.A. Macario, Removal of different dye solutions: a comparison study using a polyamide NF Membrane, Membranes 10 (12) (2020) 408.

[9] L. Wu, X. Liu, G. Lv, R. Zhu, L. Tian, M. Liu, Y. Li, W. Rao, T. Liu, L. Liao, Study on the adsorption properties of methyl orange by natural one-dimensional nano-mineral materials with different structures, Sci. Rep. 11 (1) (2021), 10640, https://doi.org/10.1038/s41598-021-90235-1.

[10] M.A. Barakat, A.Q. Selim, M. Mobarak, R. Kumar, I. Anastopoulos, D. Giannakoudakis, A. Bonilla-Petriciolet, E.A. Mohamed, M.K. Seliem, S. Komarneni, Experimental and theoretical studies of methyl orange uptake by Mn–rich synthetic mica: insights into manganese role in adsorption and selectivity, Nanomaterials 10 (8) (2020) 1464.

[11] N.S. Ali, N.M. Jabbar, S.M. Alardhi, H.S. Majdi, T.M. Albayati, Adsorption of methyl violet dye onto a prepared bio-adsorbent from date seeds: isotherm, kinetics, and thermodynamic studies, Heliyon 8 (8) (2022), e10276, https://doi.org/10.1016/j.heliyon.2022.e10276.

[12] B. Saha, A. Debnath, B. Saha, Fabrication of PANI@Fe–Mn–Zr hybrid material and assessments in sono-assisted adsorption of methyl red dye: uptake performance and response surface optimization, J. Indian Chem. Soc. 99 (9) (2022), 100635, https://doi.org/10.1016/j.jics.2022.100635.

[13] B. Saha, A. Debnath, B. Saha, Evaluation of Fe–Mn–Zr trimetal oxide/polyaniline nanocomposite as potential adsorbent for abatement of toxic dye from aqueous solution, in: A. Khadir, S.S. Muthu (Eds.), Polymer Technology in Dye-Containing Wastewater: Volume 1, Springer Nature Singapore, Singapore, 2022, pp. 15–37, https://doi.org/10.1007/978-981-19-1516-1_2.

[14] A. Deb, A. Debnath, B. Saha, Sono-assisted enhanced adsorption of eriochrome Black-T dye onto a novel polymeric nanocomposite: kinetic, isotherm, and response surface methodology optimization, J. Dispersion Sci. Technol. 42 (11) (2021) 1579–1592, https://doi.org/10.1080/01932691.2020.1775093.

[15] I. Ali, M. Asim, T.A. Khan, Low cost adsorbents for the removal of organic pollutants from wastewater, J. Environ. Manag. 113 (2012) 170–183, https://doi.org/10.1016/j.jenvman.2012.08.028.

[16] S.M. Alardhi, J.M. Alrubaye, T. Albayati, Adsorption of Methyl Green dye onto MCM-41: equilibrium, kinetics and thermodynamic studies, Desalination Water Treat. 179 (2020) 323–331.

[17] K. Mahmoudi, K. Hosni, N. Hamdi, E. Srasra, Kinetics and equilibrium studies on removal of methylene blue and methyl orange by adsorption onto activated carbon prepared from date pits-A comparative study, Kor. J. Chem. Eng. 32 (2) (2015) 274–283, https://doi.org/10.1007/s11814-014-0216-y.

[18] M. Blachnio, A. Derylo-Marczewska, B. Charmas, M. Zienkiewicz-Strzalka, V. Bogatyrov, M. Galaburda, Activated carbon from agricultural wastes for adsorption of organic pollutants, Molecules 25 (21) (2020) 5105, https://doi.org/10.3390/molecules25215105.

[19] G. Özsin, M. Kılıç, E. Apaydın-Varol, A.E. Pütün, Chemically activated carbon production from agricultural waste of chickpea and its application for heavy metal adsorption: equilibrium, kinetic, and thermodynamic studies, Appl. Water Sci. 9 (3) (2019) 56, https://doi.org/10.1007/s13201-019-0942-8.

[20] F. Ghorbani, S. Kamari, S. Zamani, S. Akbari, M. Salehi, Optimization and modeling of aqueous Cr(VI) adsorption onto activated carbon prepared from sugar beet bagasse agricultural waste by application of response surface methodology, Surface. Interfac. 18 (2020), 100444, https://doi.org/10.1016/j.surfin.2020.100444.

[21] L. Borah, M. Goswami, P. Phukan, Adsorption of methylene blue and eosin yellow using porous carbon prepared from tea waste: adsorption equilibrium, kinetics and thermodynamics study, J. Environ. Chem. Eng. 3 (2) (2015) 1018–1028, https://doi.org/10.1016/j.jece.2015.02.013.

[22] A.I. Abd-Elhamid, M. Emran, M.H. El-Sadek, A.A. El-Shanshory, H.M.A. Soliman, M.A. Akl, M. Rashad, Enhanced removal of cationic dye by eco-friendly activated biochar derived from rice straw, Appl. Water Sci. 10 (1) (2020) 45, https://doi.org/10.1007/s13201-019-1128-0.

[23] D.N. Ahmed, L.A. Naji, A.A.H. Faisal, N. Al-Ansari, M. Naushad, Waste foundry sand/MgFe-layered double hydroxides composite material for efficient removal of Congo red dye from aqueous solution, Sci. Rep. 10 (1) (2020) 2042, https://doi.org/10.1038/s41598-020-58866-y.

[24] K. Rambabu, F. Banat, G. Nirmala, S. Velu, P. Monash, G. Arthanareeswaran, Activated carbon from date seeds for chromium removal in aqueous solution, Desalination Water Treat. 156 (2019) 267–277.

[25] M. Fan, J. Hu, R. Cao, K. Xiong, X. Wei, Modeling and prediction of copper removal from aqueous solutions by nZVI/rGO magnetic nanocomposites using ANN-GA and ANN-PSO, Sci. Rep. 7 (1) (2017), 18040, https://doi.org/10.1038/s41598-017-18223-y.

[26] S. Agarwal, I. Tyagi, V.K. Gupta, M. Ghaedi, M. Masoomzade, A.M. Ghaedi, B. Mirtamizdoust, RETRACTED: kinetics and thermodynamics of methyl orange adsorption from aqueous solutions—artificial neural network-particle swarm optimization modeling, J. Mol. Liq. 218 (2016) 354–362, https://doi.org/10.1016/j.molliq.2016.02.048.

[27] M.H. Essa, Production of Activated Carbon from Date Palm Pits and its Use in Industrial Wastewater Treatment, Open University, United Kingdom, 2008.

[28] M.A. Darweesh, M.Y. Elgendy, M.I. Ayad, A.M. Ahmed, N.M.K. Elsayed, W.A. Hammad, Adsorption isotherm, kinetic, and optimization studies for copper (II) removal from aqueous solutions by banana leaves and derived activated carbon, S. Afr. J. Chem. Eng. 40 (2022) 10–20, https://doi.org/10.1016/j.sajce.2022.01.002.

[29] E.H. Khader, T.J. Mohammed, T.M. Albayati, Comparative performance between rice husk and granular activated carbon for the removal of azo tartrazine dye from aqueous solution, Desalination Water Treat. 229 (2021) 372–383.

[30] N.M. Jabbar, S.D. Salman, I.M. Rashid, Y.S. Mahdi, Removal of an anionic Eosin dye from aqueous solution using modified activated carbon prepared from date palm fronds, Chem. Data Coll. 42 (2022), 100965, https://doi.org/10.1016/j.cdc.2022.100965.

[31] S.K. Lagergren, About the theory of so-called adsorption of soluble substances, Sven. Vetenskapsakad. Handingarl 24 (1898) 1–39.

[32] Y.-S. Ho, G. McKay, Pseudo-second order model for sorption processes, Process Biochem. 34 (5) (1999) 451–465.

[33] M. Ghaedi, A.M. Ghaedi, A. Ansari, F. Mohammadi, A. Vafaei, Artificial neural network and particle swarm optimization for removal of methyl orange by gold nanoparticles loaded on activated carbon and Tamarisk, Spectrochim. Acta Mol. Biomol. Spectrosc. 132 (2014) 639–654, https://doi.org/10.1016/j.saa.2014.04.175.

[34] M. Tanzifi, S.H. Hosseini, A.D. Kiadehi, M. Olazar, K. Karimipour, R. Rezaiemehr, I. Ali, Artificial neural network optimization for methyl orange adsorption onto polyaniline nano-adsorbent: kinetic, isotherm and thermodynamic studies, J. Mol. Liq. 244 (2017) 189–200, https://doi.org/10.1016/j.molliq.2017.08.122.

[35] B. Tanhaei, A. Ayati, M. Lahtinen, B.M. Vaziri, M. Sillanpää, A magnetic mesoporous chitosan based core shells biopolymer for anionic dye adsorption: kinetic and isothermal study and application of ANN, J. Appl. Polym. Sci. 133 (2016).

[36] I. Salehi, M. Shirani, A. Semnani, M. Hassani, S. Habibollahi, Comparative study between response surface methodology and artificial neural network for adsorption of crystal violet on magnetic activated carbon, Arabian J. Sci. Eng. 41 (7) (2016) 2611–2621, https://doi.org/10.1007/s13369-016-2109-3.

[37] N.M. Mahmoodi, Z. Hosseinabadi-Farahani, F. Bagherpour, M.R. Khoshrou, H. Chamani, F. Forouzeshfar, Synthesis of CuO–NiO nanocomposite and dye adsorption modeling using artificial neural network, Desalination Water Treat. 57 (37) (2016) 17220–17229, https://doi.org/10.1080/19443994.2015.1086895.

[38] B. Heibati, S. Rodriguez-Couto, O. Ozgonenel, N.G. Turan, A. Aluigi, M.A. Zazouli, M.G. Ghozikali, M. Mohammadyan, A.B. Albadarin, A modeling study by artificial neural network on ethidium bromide adsorption optimization using natural pumice and iron-coated pumice, Desalination Water Treat. 57 (29) (2016) 13472–13483, https://doi.org/10.1080/19443994.2015.1060906.

[39] M. Ghaedi, A.M. Ghaedi, A. Ansari, F. Mohammadi, A. Vafaei, Artificial neural network and particle swarm optimization for removal of methyl orange by gold nanoparticles loaded on activated carbon and Tamarisk, Spectrochim. Acta Mol. Biomol. Spectrosc. 132 (2014) 639–654, https://doi.org/10.1016/j.saa.2014.04.175.
[40] A.A. Babaei, A. Khataee, E. Ahmadpour, M. Sheydaei, B. Kakavandi, Z. Alaee, Optimization of cationic dye adsorption on activated spent tea: equilibrium, kinetics, thermodynamic and artificial neural network modeling, Kor. J. Chem. Eng. 33 (4) (2016) 1352–1361, https://doi.org/10.1007/s11814-014-0334-6.
[41] R. Krishnamoorthy, B. Govindan, F. Banat, V. Sagadevan, M. Purushothaman, P.L. Show, Date pits activated carbon for divalent lead ions removal, J. Biosci. Bioeng. 128 (1) (2019) 88–97, https://doi.org/10.1016/j.jbiosc.2018.12.011.
[42] A.K. Mallick, A. Jha, B.P. Pokharel, R. Rajbhandari, R.M. Shrestha, Activated carbons derived from date (phoenix dactylifera) seeds with excellent iodine adsorption properties, J. Inst. Eng. (2019).
[43] E. Rápó, S. Tonk, Factors affecting synthetic dye adsorption; desorption studies: a review of results from the last five years (2017-2021), Molecules 26 (17) (2021) 5419, https://doi.org/10.3390/molecules26175419.
[44] P. Das, P. Debnath, A. Debnath, Enhanced sono-assisted adsorptive uptake of malachite green dye onto magnesium ferrite nanoparticles: kinetic, isotherm and cost analysis, Environ. Nanotechnol. Monit. Manag. 16 (2021), 100506, https://doi.org/10.1016/j.enmm.2021.100506.
[45] T. Santhi, S. Manonmani, T. Smitha, Removal of methyl red from aqueous solution by activated carbon prepared from the Annona squmosa seed by adsorption, Chem. Eng. Res. Bull. 14 (1) (2010) 11–18, https://doi.org/10.3329/cerb.v14i1.3767.
[46] H.A. Abdulhussein, A.A. Hassan, Methyl red dye removal from aqueous solution by adsorption on rice hulls, Babylon Univ. Sci 23 (2015) 627–637.
[47] F. Gorzin, M.M. Bahri Rasht Abadi, Adsorption of Cr(VI) from aqueous solution by adsorbent prepared from paper mill sludge: kinetics and thermodynamics studies, Adsorpt. Sci. Technol. 36 (1–2) (2017) 149–169, https://doi.org/10.1177/0263617416686976.
[48] A.A. Alghamdi, A.B. Al-Odayni, W.S. Saeed, A. Al-Kahtani, F.A. Alharthi, T. Aouak, Efficient adsorption of lead (II) from aqueous phase solutions using polypyrrole-based activated carbon, Materials 12 (12) (2019), https://doi.org/10.3390/ma12122020.
[49] Y. El Maguana, N. Elhadiri, M. Bouchdoug, M. Benchanaa, A. Jaouad, Activated carbon from prickly pear seed cake: optimization of preparation conditions using experimental design and its application in dye removal, Int. J. Chem. Eng. 2019 (2019), 8621951, https://doi.org/10.1155/2019/8621951.
[50] S. Rattanapan, J. Srikram, P. Kongsune, Adsorption of methyl orange on coffee grounds activated carbon, Energy Proc. 138 (2017) 949–954, https://doi.org/10.1016/j.egypro.2017.10.064.
[51] Y. Yu, N. Qiao, D. Wang, Q. Zhu, F. Fu, R. Cao, R. Wang, W. Liu, B. Xu, Fluffy honeycomb-like activated carbon from popcorn with high surface area and well-developed porosity for ultra-high efficiency adsorption of organic dyes, Bioresour. Technol. 285 (2019), 121340, https://doi.org/10.1016/j.biortech.2019.121340.
[52] M.T. Islam, R. Saenz-Arana, C. Hernandez, T. Guinto, M.A. Ahsan, D.T. Bragg, H. Wang, B. Alvarado-Tenorio, J.C. Noveron, Conversion of waste tire rubber into a high-capacity adsorbent for the removal of methylene blue, methyl orange, and tetracycline from water, J. Environ. Chem. Eng. 6 (2) (2018) 3070–3082, https://doi.org/10.1016/j.jece.2018.04.058.